

Covariant propagator of the Rarita-Schwinger field in the nuclear medium

C.L. Korpa

Department of Theoretical Physics, University of Pécs, H-7624 Pécs, Hungary

A.E.L. Dieperink

KVI, Zernikelaan 25, NL-9747AA Groningen, The Netherlands

(Dated: September 2, 2021)

A formalism for representing the fully relativistic propagator of the Rarita-Schwinger field in the nuclear medium is developed. Using a convenient basis for expanding the propagator it is shown that it can be represented by 40 energy and momentum dependent quantities which can be decomposed into an 2×2 and an 6×6 matrix. In this way calculations reduce to matrix multiplication. Using the presented formalism the full relativistically covariant contribution of the pion-nucleon loop to the isobar self energy and propagator in isospin-symmetric spin-saturated nuclear medium is computed. Utilizing this propagator the photoabsorption cross-section on in-medium nucleons in the isobar region is calculated and the result compared with experimental data.

PACS numbers: 25.20.Dc, 24.10.Jv, 21.65.+f

I. INTRODUCTION

The spin-3/2 isospin-3/2 $\Delta(1232)$ baryon (in the following referred to as the isobar and denoted by Δ) couples strongly to the nucleon and pion and plays an important role in nuclear processes with excitation energy of a few hundred MeV. This raises the issue of the propagation of a spin-3/2 particle in the nuclear medium. The spin-3/2 particle is usually described by using the Rarita-Schwinger field [1], which consists of four, Lorentz-vector indexed, Dirac spinors. A free theory can be formulated in which the number of degrees of freedom is as a consequence of the equations of motion reduced to the required 8 (for a complex field). However, for realistic description of spin-3/2 resonances one needs to introduce interactions taking into account their decay channels.

Introducing interactions of general form into the above free-field theory introduces also spin-1/2 components into the propagator. This type of approach was used quite extensively in the past for the delta baryon and was phenomenologically successful (see, for example, Ref. [2]). Recently it has been argued [3, 4] that an interaction vertex which preserves the correct number of degrees of freedom for the spin-3/2 particle should be used. It has been also shown [5] that the two types of couplings can be transformed into each other by a redefinition of the field describing the spin-3/2 particle, at the expense of new contact interactions appearing (not containing the spin-3/2 field) in the lagrangian. These contact interactions may be associated with other spin-1/2 fields in the theory.

The propagator we are interested in is defined by

$$G^{\mu\nu}(p) = i \int d^4x e^{ip \cdot x} \langle 0 | T \Psi^\mu(x) \bar{\Psi}^\nu(0) | 0 \rangle, \quad (1)$$

where Ψ^μ is the Rarita-Schwinger field and $|0\rangle$ can denote either the vacuum or the nuclear medium. In vacuum this propagator (or the self energy, which is given by the amputated diagrams of (1)) can be expanded in terms of 10 Lorentz-scalar functions of p^2 . This number can easily be understood if we count the number of terms corresponding to the Lorentz structure given by Eq. (1). Indeed, the two vector indices can be represented by the 5 terms $g^{\mu\nu}, p^\mu p^\nu, p^\mu \gamma^\nu, \gamma^\mu p^\nu, \gamma^\mu \gamma^\nu$ (γ^μ are the Dirac matrices); these are multiplied by the 4×4 unit matrix, $\mathbb{1}$, or the contraction $\not{p} \equiv p_\alpha \gamma^\alpha$.

In the nuclear medium the propagator acquires more independent components than in vacuum, since the presence of the (rotationally symmetric) medium means that preserving the Lorentz-covariant description requires introducing another four-vector, namely the medium's four velocity. This quadruples the number of terms the propagator can be expanded in (see section II for details). To our knowledge a complete calculation involving all these terms has not been carried out and either a nonrelativistic approach (for example as in Ref. [6]), a description based on combining off-shell and on-shell behavior [7], or a treatment based on the assumption that the isobar propagator is proportional to the spin-3/2 projector [8, 9] was used. The implications of this latter approach we discuss in some detail in the subsection II B. Our aim is to provide a general scheme for a fully Lorentz-covariant treatment of the spin-3/2 particle's in-medium propagation, analitically separating all its components. This means introducing a convenient basis for the expansion of the self energy and the propagator, which makes subsequent calculations practical for arbitrary vertices involving the Rarita-Schwinger field.

In the first part of section II we develop the general formalism for a covariant treatment of the spin-3/2 field in the nuclear medium, while in the second part we provide numerical results for the in-medium delta propagator. In section III we calculate the total cross section for the nuclear photoabsorption and compare the results with observations.

II. RELATIVISTIC PROPAGATOR OF THE IN-MEDIUM RARITA-SCHWINGER FIELD

A. Formalism

To exhibit the general Lorentz-structure of the spin-3/2 particle's propagator and self energy in the medium, we observe that in the presence of rotationally symmetric nuclear medium the latter's state of motion is given by its four-velocity, $u^\mu \equiv 1/\sqrt{1-\vec{v}^2/c^2}(1, \vec{v}/c)$. This implies that in addition to the 5 objects with two Lorentz-vector indices in vacuum (see the preceding section), we get 5 more: $u^\mu p^\nu, p^\mu u^\nu, u^\mu \gamma^\nu, \gamma^\mu u^\nu, u^\mu u^\nu$. Also, the 4×4 matrices \not{u} and \not{p} , in addition to $\mathbb{1}$ and \not{p} appear, producing in all 40 terms of the basis.

While in vacuum one may argue that the definite spin of the particle restricts the form of the propagator and decreases the number of the nonzero expansion coefficients, in medium such an argument is meaningless. The reason is that, even in a rotationally symmetric medium, the spin of a particle moving with respect to the medium is not a good quantum number, since the momentum of the particle (in the rest frame of the medium) defines a preferred direction and only rotations about that axis are a symmetry transformation. This means that only the projection of the angular momentum on the momentum, i.e. helicity, is a good quantum number. As a consequence, not only spin-3/2 and spin-1/2 components, but also those corresponding to mixing of these spins should in general appear in the propagator, with the restriction that helicity-1/2 and helicity-3/2 states do not mix. We remark that the sign of the helicity does not matter, since parity is a symmetry operation.

A convenient basis containing the 40 terms mentioned above has actually been constructed in Ref. [10], when an in-medium generalization of the partial-wave expansion has been introduced. In that case a basis for s-, p- and d-waves with $J = 1/2$ and $J = 3/2$ (including their mixing) was obtained, containing 68 terms. Of these only 40 terms are relevant for the present case, since the rest does not have two Lorentz-vector indices.

To introduce the relevant basis we recapitulate the definition and basic properties of its building blocks. First, the terms P_\pm and U_\pm are introduced¹ providing the 4×4 matrix structure, by the relations:

$$P_\pm(p) = \frac{1}{2} \left(1 \pm \frac{\not{p}}{\sqrt{p^2}} \right), \quad U_\pm(p, u) = -P_\pm(p) \frac{i \gamma \cdot u}{\sqrt{(p \cdot u)^2/p^2 - 1}} P_\mp(p). \quad (2)$$

They have the following multiplication properties:

$$\begin{aligned} P_\pm P_\pm &= P_\pm = U_\pm U_\mp, & P_\pm P_\mp &= 0 = U_\pm U_\pm, \\ P_\pm U_\pm &= U_\pm = U_\pm P_\mp, & P_\pm U_\mp &= 0 = U_\pm P_\pm. \end{aligned} \quad (3)$$

One can observe that on-shell the $P_\pm(p)$ are the positive- and negative-energy projectors.

To exhibit the remaining rotational symmetry in the medium, leading to the conservation of helicity, it is advantageous to use, apart from p^μ , the following four quantities [10]:

$$\begin{aligned} V_\mu(p) &= \frac{1}{\sqrt{3}} \left(\gamma_\mu - \frac{\not{p}}{p^2} p_\mu \right), & X_\mu(p, u) &= \frac{(p \cdot u) p_\mu - p^2 u_\mu}{p^2 \sqrt{(p \cdot u)^2/p^2 - 1}}, \\ R_\mu(p, u) &= \frac{1}{\sqrt{2}} \left(U_+(p, u) + U_-(p, u) \right) V_\mu(p) - i \sqrt{\frac{3}{2}} X_\mu(p, u), \\ L_\mu(p, u) &= \frac{1}{\sqrt{2}} V_\mu(p) \left(U_+(p, u) + U_-(p, u) \right) - i \sqrt{\frac{3}{2}} X_\mu(p, u), \end{aligned} \quad (4)$$

While they are not all independent, they are constructed in such a way to make the basis orthogonal, see Eq. (8) below, and are motivated by the helicity basis for the partial-wave expansion [10].

¹ In Ref. [10] due to typographical errors in Eq. (A1) a minus sign is missing in the defining expression for U_\pm , and also the sign of the terms containing $U_+(w, u) + U_-(w, u)$ in equations defining R_μ and L_μ should be changed.

It turns out that the basis can be constructed in such a way that the multiplication algebra of its 40 objects separates into two subalgebras, one containing 4 and the other 36 terms. The existence of two separate subalgebras of the expansion basis is explained by the helicity conservation in the medium. The 4 terms of the first subalgebra can be cast in the form of a 2×2 matrix, which corresponds to helicity-3/2 components, containing the positive-energy and negative-energy states (and their mixing). The remaining 36 terms, suitably grouped in a 6×6 matrix, describe the helicity-1/2 components. They come from the spin-3/2 part of the Rarita-Schwinger field and the two spin-1/2 sectors present in that field, and positive and negative energy components for each of the above mentioned spin sectors.

The 4 terms of the first subalgebra are given by $Q_{[ij]}^{\mu\nu}$ with $i, j = 1, 2$, defined as follows:

$$\begin{aligned}
Q_{[11]}^{\mu\nu} &= \left(g^{\mu\nu} - \hat{p}^\mu \hat{p}^\nu \right) P_+ - V^\mu P_- V^\nu - L^\mu P_+ R^\nu, \\
Q_{[22]}^{\mu\nu} &= \left(g^{\mu\nu} - \hat{p}^\mu \hat{p}^\nu \right) P_- - V^\mu P_+ V^\nu - L^\mu P_- R^\nu, \\
Q_{[12]}^{\mu\nu} &= \left(g^{\mu\nu} - \hat{p}^\mu \hat{p}^\nu \right) U_+ + \frac{1}{3} V^\mu U_- V^\nu \\
&\quad + \frac{\sqrt{8}}{3} \left(L^\mu P_+ V^\nu + V^\mu P_- R^\nu \right) - \frac{1}{3} L^\mu U_+ R^\nu, \\
Q_{[21]}^{\mu\nu} &= \left(g^{\mu\nu} - \hat{p}^\mu \hat{p}^\nu \right) U_- + \frac{1}{3} V^\mu U_+ V^\nu \\
&\quad + \frac{\sqrt{8}}{3} \left(L^\mu P_- V^\nu + V^\mu P_+ R^\nu \right) - \frac{1}{3} L^\mu U_- R^\nu,
\end{aligned} \tag{5}$$

where $\hat{p}_\mu = p_\mu / \sqrt{p^2}$.

The 36 components $P_{[ij]}^{\mu\nu}$ of the second subalgebra are given by the relation:

$$P_{[ij]}^{\mu\nu} = P_i^\mu \bar{P}_j^\nu, \quad i, j = 1, \dots, 6, \tag{6}$$

where:

$$\begin{aligned}
P_1^\mu &= V_\mu P_+, \quad \bar{P}_1^\mu = P_+ V^\mu, \\
P_2^\mu &= V_\mu U_-, \quad \bar{P}_2^\mu = U_+ V^\mu, \\
P_3^\mu &= \hat{p}_\mu P_+, \quad \bar{P}_3^\mu = P_+ \hat{p}^\mu, \\
P_4^\mu &= \hat{p}_\mu U_-, \quad \bar{P}_4^\mu = U_+ \hat{p}^\mu, \\
P_5^\mu &= L_\mu P_+, \quad \bar{P}_5^\mu = P_+ R^\mu, \\
P_6^\mu &= L_\mu U_-, \quad \bar{P}_6^\mu = U_+ R^\mu.
\end{aligned} \tag{7}$$

The $Q_{[ij]}^{\mu\nu}$ and $P_{[ij]}^{\mu\nu}$ satisfy the following relations:

$$\begin{aligned}
Q_{[ik]}^{\mu\alpha} g_{\alpha\beta} P_{[lj]}^{\beta\nu} &= 0 = P_{[ik]}^{\mu\alpha} g_{\alpha\beta} Q_{[lj]}^{\beta\nu}, \\
Q_{[ik]}^{\mu\alpha} g_{\alpha\beta} Q_{[lj]}^{\beta\nu} &= \delta_{kl} Q_{[ij]}^{\mu\nu}, \quad P_{[ik]}^{\mu\alpha} g_{\alpha\beta} P_{[lj]}^{\beta\nu} = \delta_{kl} P_{[ij]}^{\mu\nu}.
\end{aligned} \tag{8}$$

The free and the dressed propagator, as well as the self energy of the Rarita-Schwinger field can be expanded in the basis spanned by $Q_{[ij]}^{\mu\nu}$ and $P_{[ij]}^{\mu\nu}$:

$$G_0^{\mu\nu}(p) = \sum_{i,j=1}^2 Q_{[ij]}^{\mu\nu} g_{[ij]}^{(Q)}(p) + \sum_{i,j=1}^6 P_{[ij]}^{\mu\nu} g_{[ij]}^{(P)}(p), \tag{9a}$$

$$G^{\mu\nu}(p, u) = \sum_{i,j=1}^2 Q_{[ij]}^{\mu\nu} G_{[ij]}^{(Q)}(p, u) + \sum_{i,j=1}^6 P_{[ij]}^{\mu\nu} G_{[ij]}^{(P)}(p, u), \tag{9b}$$

$$\Sigma^{\mu\nu}(p, u) = \sum_{i,j=1}^2 Q_{[ij]}^{\mu\nu} \sigma_{[ij]}^{(Q)}(p, u) + \sum_{i,j=1}^6 P_{[ij]}^{\mu\nu} \sigma_{[ij]}^{(P)}(p, u), \tag{9c}$$

where the dependence of $Q_{[ij]}^{\mu\nu}$ and $P_{[ij]}^{\mu\nu}$ on p and u is not shown. Using the orthogonality relations (8) the Dyson equation

$$G^{\mu\nu} = G_0^{\mu\nu} + G_0^{\mu\alpha} g_{\alpha\beta} \Sigma^{\beta\gamma} g_{\gamma\delta} G^{\delta\nu} \tag{10}$$

simply becomes a matrix equation, where the matrices are constructed from the corresponding expansion coefficients $c_{[ij]}$, with i being the row index, j the column index:

$$\begin{aligned} G_{[ij]}^{(Q)} &= g_{[ij]}^{(Q)} + \sum_{k,\ell=1}^2 g_{[ik]}^{(Q)} \sigma_{[k\ell]}^{(Q)} G_{[\ell j]}^{(Q)}, \\ G_{[ij]}^{(P)} &= g_{[ij]}^{(P)} + \sum_{k,\ell=1}^6 g_{[ik]}^{(P)} \sigma_{[k\ell]}^{(P)} G_{[\ell j]}^{(P)}. \end{aligned} \quad (11)$$

This means we can simply solve for the expansion functions of the propagator:

$$\tilde{G}^{(A)} = (\tilde{g}^{(A)-1} - \tilde{\sigma}^{(A)})^{-1}, \quad (12)$$

with $A = Q, P$ and \tilde{G} denoting a matrix with elements $G_{[ij]}$.

B. Relativistic propagator of the isobar

We start from the free isobar propagator in its standard form

$$G_0^{\mu\nu}(p) = \frac{\not{p} + M_\Delta}{p^2 - M_\Delta^2 + i\varepsilon} \left[g^{\mu\nu} - \frac{\gamma^\mu \gamma^\nu}{3} - \frac{2p^\mu p^\nu}{3M_\Delta^2} + \frac{p^\mu \gamma^\nu - p^\nu \gamma^\mu}{3M_\Delta} \right]. \quad (13)$$

The expansion coefficients of its inverse can be simply calculated by matrix inversion and are given in Appendix A.

The self energy of the isobar close to its on-shell energy is dominated by the pion-nucleon loop and for the relevant pion-nucleon-isobar coupling we use the expression

$$\mathcal{L}_{\pi N \Delta} = g_{\pi N \Delta} \partial_\alpha \pi \bar{\Delta}_\beta (g^{\alpha\beta} + a \gamma^\beta \gamma^\alpha) N + \text{h.c.} \quad (14)$$

An explicit computation in vacuum based on the coupling (14) showed [11] that by introducing a pion-nucleon-isobar form factor depending on the square of isobar's 4-momentum (since the pion and the nucleon are on-shell), an excellent fit to the pion-nucleon scattering phase shift in the isospin-3/2 spin-3/2 channel is possible, up to the pion laboratory momentum of 500 MeV, by adjusting the coupling, the isobar's bare mass and the cut-off in the form factor. The off-shell parameter a , as expected, does not play a significant role in the energy range of interest. Also, that calculation showed that the spin-1/2 components of the isobar spectral function are about two orders of magnitude smaller than the spin-3/2 ones in the resonance region. The Rarita-Schwinger propagator in vacuum was recently discussed in Ref. [12], where some elements of the basis used in the present approach were introduced (of course, without the terms relevant for the nuclear medium).

For the in-medium calculation of the isobar self energy we also use the interaction lagrangian (14), but with the off-shell parameter a put to zero. This is mainly done for simplicity and is motivated by the observation of Ref. [11] that this parameter has a very small effect on the isobar propagator (in vacuum) in the resonance region, i.e. not far off-shell. The coefficients of the self-energy expansion are given in Appendix A, Eq. (A2), together with the definition of the pion-nucleon loop integrals appearing in those functions. These loop integrals correspond to the ones defined in Ref. [10] for the case of kaon-nucleon scattering.

For a comparison with the result of the non-relativistic approach we calculated the isobar propagator using the pion spectral function and the $\pi N \Delta$ coupling and form factor of Ref. [6]. We observe that two entries in the propagator, one in $\tilde{G}^{(Q)}$ and one in $\tilde{G}^{(P)}$, are much larger than any of the remainder, which brings us again to the interpretation of these matrix elements. As discussed in the previous subsection, the appearance of the block diagonal structure, i.e. matrices with superscripts Q and P , is a reflection of the fact that helicity is still a good quantum number and consequently different helicity states do not mix. The 2×2 matrix contains the helicity-3/2 components (see also Ref. [10]) of the positive and negative energy states and their mixing. The [11] element of this matrix is much larger (for positive energies) than the others and is referred to as the helicity-3/2 component of the in-medium isobar. We repeat that the projector P_+ appearing in this term when on-shell, i.e. for $p^2 = M^2$, is the positive energy projector.

The matrix $\tilde{G}^{(P)}$ contains the helicity-1/2 components, of both spin-1/2 and spin-3/2 (which mix), and positive-energy and negative-energy components. The element [55] of this matrix is the dominant one and is identified with the spin-3/2 term (also positive energy). The appearance of the 6×6 matrix structure, and not a 4×4 one, is a consequence of the number of degrees of freedom of the Rarita-Schwinger field, which means that there are two spin-1/2 sectors in that field.

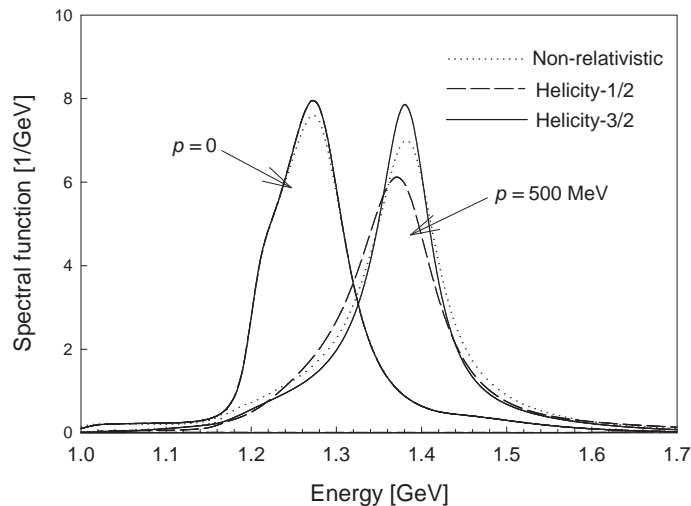


FIG. 1: The isobar spectral function in the nuclear medium at saturation density and momentum $|\vec{p}| = 0$ and $|\vec{p}| = 500$ MeV. The pion spectral function and the $\pi N\Delta$ form factor, as well as the dotted line result for the isobar spectral function are from a non-relativistic calculation of Ref.[6]. At zero momentum the two different helicity curves coincide, while at $|\vec{p}| = 500$ MeV there is a clear distinction.

In Fig. 1 we show the spectral functions of the helicity-1/2 and helicity-3/2 isobar states, i.e. $-\text{Im} G_{[55]}^{(P)}/\pi$ and $-\text{Im} G_{[11]}^{(Q)}/\pi$, in isospin-symmetric nuclear matter with Fermi momentum $k_F = 270$ MeV, at momentum 0 and 500 MeV. For comparison we also show the results of the non-relativistic calculation of Ref. [6], when the isobar propagator has only one component.

The spectral functions of all the other components are significantly smaller than the ones shown in Fig. 1 and for the considered density and for isobar momentum less than 1 GeV they do not exceed few percent of the dominant spectral functions, if considering the resonance region. This implies that we can obtain practically the same results by calculating only two components of the propagator and that these can be obtained from only two components of the self energy. In vacuum it suffices to calculate only one component (say $\sigma_{[11]}^{(Q)}$) of the self energy and then the corresponding propagator to perform a relativistic treatment with few-percent accuracy.

We now want to clarify the content of the schemes used in Refs. [8, 9], where the assumption is made that the in-medium isobar propagator is proportional to the spin-3/2 projector. The latter can be written through the terms of our basis introduced in Eqs. (5) and (6) as:

$$P_{3/2}^{\mu\nu} = Q_{[11]}^{\mu\nu} + Q_{[22]}^{\mu\nu} + P_{[55]}^{\mu\nu} + P_{[66]}^{\mu\nu}, \quad (15)$$

corresponding to positive-energy and negative-energy helicity-3/2 and helicity-1/2 terms of the spin-3/2 sector. If one multiplies Eq. (15) with $a\not{p} + b\mathbb{1}$ (on the left or the right) to get the complete expression for the propagator (as done in Refs. [8, 9]), only the positive-energy and negative-energy content will change, while the coefficients giving the helicity-1/2 and helicity-3/2 components necessarily remain the same. In this way the splitting between different helicity states of the spin-3/2 sector is neglected in the approach mentioned, which is in this respect reminiscent of the non-relativistic treatment (however, keeping both positive-energy and negative-energy contributions). We stress that this is not equivalent (in the medium) to using the general form of the propagator and then applying the projector (15), which would take into account the helicity splitting.

III. NUCLEAR PHOTOABSORPTION IN THE ISOBAR REGION

We now turn to the photon absorption cross section on a nucleon in the isobar region, i.e. for photon energies between 0.2 and 0.5 GeV. First we consider the free nucleon case and subsequently that of a large nucleus, whose

nucleons and the isobar are modelled by their nuclear matter properties.

We start with the absorption of the photon by a free nucleon. As a consequence of the unitarity of the S matrix the total photon-absorption cross section on the nucleon is proportional to the imaginary part of the photon-nucleon forward-scattering amplitude,

$$\sigma_T = \frac{1}{2M_N q_0} \text{Im } A_{\gamma N}, \quad (16)$$

where we work in the rest frame of the nucleon and q_0 is the photon energy in that frame.

For the $\gamma N\Delta$ vertex we use the dominant magnetic dipole term [13]:

$$\mathcal{L}_{\gamma N\Delta} = \frac{3e}{2M_N(M_N + M_\Delta)} i g_m \bar{N} T_3^\dagger \tilde{F}^{\mu\nu} \partial_\mu \Delta_\nu + \text{h.c.}, \quad (17)$$

where $\tilde{F}_{\mu\nu} \equiv \varepsilon_{\mu\nu\alpha\beta} F^{\alpha\beta}/2$ and $F_{\mu\nu} \equiv \partial_\mu A_\nu - \partial_\nu A_\mu$, with A_μ being the electromagnetic field and g_m a dimensionless number giving the strength of the transition. The photon-nucleon forward-scattering amplitude through the isobar intermediate state for arbitrary q photon 4-momentum and k nucleon 4-momentum becomes:

$$A_{\gamma N}(q, k) = \frac{2}{3} \frac{1}{4} \text{Tr} \left[(\not{k} + M_N) \Gamma_\alpha^\mu(k, q) G^{\alpha\beta}(q+k) \Gamma_{\beta\mu}(k, q) \right], \quad (18)$$

where the factor $1/4$ comes from averaging over the spin of the nucleon and photon polarization, and

$$\Gamma_{\mu\nu}(k, q) \equiv \frac{3e}{2M_N(M_N + M_\Delta)} g_m \varepsilon_{\mu\nu\alpha\beta} k^\alpha q^\beta.$$

Inserting the expansion of the isobar propagator (9b) and calculating the trace we arrive at the forward-scattering amplitude in the form

$$A_{\gamma N}(q, k) = \frac{1}{3} g_m^2 h_m^2 \left(\sum_{i,j=1}^2 a_{[ij]}^{(Q)}(k, q) G_{[ij]}^{(Q)}(q+k) + \sum_{i,j=1}^6 a_{[ij]}^{(P)}(k, q) G_{[ij]}^{(P)}(q+k) \right), \quad (19)$$

where

$$h_m \equiv \frac{3e}{2M_N(M_N + M_\Delta)},$$

and the expressions for $a_{[ij]}^{(Q)}(k, q)$ and $a_{[ij]}^{(P)}(k, q)$ are given in the Appendix B, and $G_{[ij]}^{(Q)}(q+k)$ and $G_{[ij]}^{(P)}(q+k)$ are the expansion coefficients of the isobar propagator, as defined by Eq. (9b).

The calculated cross section is shown in Fig. 2, where the dressed isobar propagator in vacuum is calculated using the free propagators of the nucleon and pion. For the $\pi N\Delta$ form factor we used an exponential function of the isobar's 4-momentum p :

$$F_{\pi N\Delta}(p^2) = \exp \left[- (p^2 - (m_N + m_\pi)^2) / \Lambda^2 \right], \quad (20)$$

which has been fitted to reproduce the pion-nucleon scattering phase shift in the isobar channel up to pion laboratory momentum of 500 MeV [11], leading to $\Lambda = 0.97$ GeV and the $\pi N\Delta$ coupling multiplying Eq. (20), $g_{\pi N\Delta} = 20.2$ GeV⁻¹. The solid line in Fig. 2 is obtained without introducing a form factor for the $\gamma N\Delta$ vertex, although the coupling (17) allows it without affecting the conservation of the current to which the photon field couples. The dashed line corresponds to the $\gamma N\Delta$ form factor used in Ref. [8]. As one can see in the energy region of interest the effect of the form factor is rather small. The points with error bars show measurement results from Ref. [14], where we did not attempt to subtract the background in view of its uncertainty [14].

The only terms giving significant contributions in the sum of Eq. (19) are those containing $G_{[11]}^{(Q)}(p)$ and $G_{[55]}^{(P)}(p)$, where we find numerically that the first one gives three times the contribution of the second. This confirms the interpretation of the $G_{[11]}^{(Q)}(p)$ as corresponding to helicity 3/2 and $G_{[55]}^{(P)}(p)$ to helicity 1/2, since for a magnetic dipole transition the $\gamma N \rightarrow \Delta$ amplitudes in the isobar helicity basis are related by a factor of $\sqrt{3}$ [15].

We now turn to the nuclear medium. Modification of the following ingredients of the calculation can be expected: the nucleon spectral function, the delta spectral function and the $\gamma N\Delta$ vertex. For the nucleons we use the Fermi-gas approximation, which means that we neglect the small broadening of the nucleon-hole spectral function, but take care

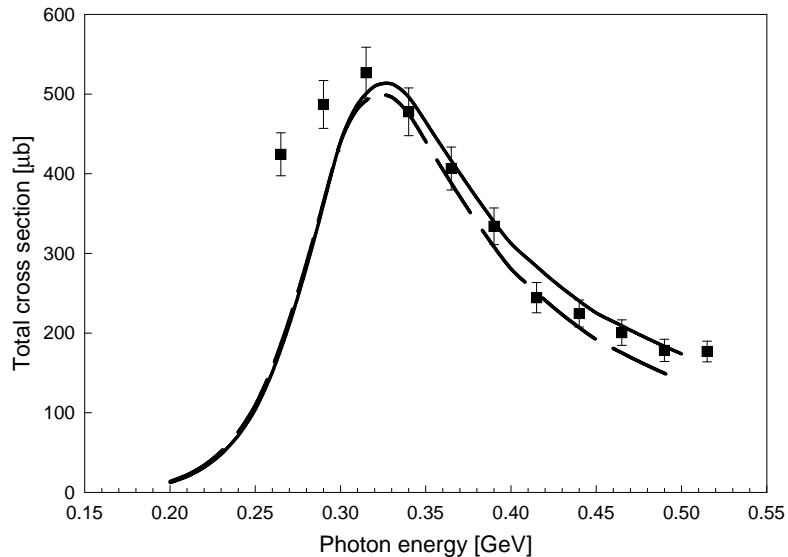


FIG. 2: The total photoabsorption cross section on free nucleon, with the isobar propagator taken from Ref. [11]. The calculation leading to the solid line is based on magnetic-dipole $\gamma N\Delta$ vertex without form factor, with coupling $g_m = 3$. The dashed line shows the effect of the form factor used in Ref. [8].

of its Fermi motion which contributes significantly to the broadening of the cross-section energy distribution. The small shift of the spectral-function peak due to binding we accommodate by allowing a mean-field shift of the isobar's mass, since only the difference of the two values plays a role. The main effect of the medium (apart from the nucleon's Fermi motion) comes from the modified isobar propagator which we compute using an in-medium pion propagator. To assure a reasonable width of the isobar it is necessary to include a rather soft $\pi N\Delta$ form factor in this calculation, giving support to previous conclusions about its strong momentum dependence [16]. For the $\gamma N\Delta$ vertex we assume absence of medium modification.

The pion propagator in the nuclear medium acquires properties distinguishing it significantly from the vacuum case [6, 8, 17, 18]. The particle-hole excitation introduces a spectral-function strength at low energy, while the isobar-hole one gives a finite width to the main peak and gives rise to the isobar-hole branch at energies above the central maximum (with which it can merge). The quantitative result for the in-medium propagator depends sensitively on the pion-nucleon-nucleon and pion-nucleon-isobar form factor used, as well as on the values of the Migdal's g' parameters ($g'_{NN}, g'_{N\Delta}, g'_{\Delta\Delta}$). The low-energy strength in the pion spectral function and the broadening of the main maximum, usually accompanied with a shift toward smaller energy, enhance the decay width of the isobar into a nucleon and pion, while the Pauli blocking decreases the decay probability. The last mechanism is effective only at small isobar momenta. In self-consistent calculations (or in ones using a dressed pion) this pronounced broadening of the isobar can cause problems. In Ref. [8] a large mean-field shift of the isobar energy was used to suppress this unwelcome result, while in Ref. [6] the pion-momentum dependent $\pi N\Delta$ form factor achieved the same effect.

Our point of view is that it is plausible to use a suitable form factor which suppresses the far off-shell (with energy around zero and momentum of few hundred MeV) pion contribution to the isobar self energy and in the following we applied this strategy. This is corroborated by considerations of deep inelastic scattering on nucleon in the pion-cloud model [16], where the pion can be far off-shell, and soft πNN and $\pi N\Delta$ form factors prevent overestimation of antiquark distributions. To be consistent with the vacuum calculation of the isobar self energy, we introduce an (exponential) form factor depending on the pion 4-momentum squared (which reduces to unity for an on-shell pion):

$$f_{\pi N\Delta}(q_\pi^2) = \exp \left[-(q_\pi^2 - m_\pi^2)^2 / \Lambda_{\pi N\Delta}^4 \right]. \quad (21)$$

Expression (21) multiplies Eq. (20) to give the full $\pi N\Delta$ form factor:

$$\tilde{F}_{\pi N\Delta}(p^2, q_\pi^2) = F_{\pi N\Delta}(p^2) \cdot f_{\pi N\Delta}(q_\pi^2). \quad (22)$$

We remark that a hard form factor depending on q_π^2 was introduced also in Ref. [8], but it did not provide a significant suppression of the off-shell pion contribution. The parameter $\Lambda_{\pi N\Delta}$ is expected to be of the order of a few m_π .

In order to be able to take into account the Fermi motion of the nucleons we start with the photon-absorption cross

section on a nucleon moving with momentum \vec{k} :

$$\sigma_T(k, q) = \frac{1}{2q_0 [E_N(\vec{k}) - |\vec{k}| \cos \theta]} \text{Im } A_{\gamma N}(q, k), \quad (23)$$

where q is the photon's 4-momentum and θ is the angle between the photon and nucleon 3-momenta. The expression (19) for the forward-scattering amplitude and the coefficient functions $a_{[ij]}^{(Q)}(k, q)$ and $a_{[ij]}^{(P)}(k, q)$ are general and apply also in this case. The numerical computation is performed in the rest frame of the medium and involves averaging over the nucleon's momentum:

$$\sigma_T(q_0) = \frac{4}{\rho} \int_0^{k_F} \frac{k^2 dk}{(2\pi)^2} \int_{-1}^1 d\mu \sigma_T(q, k), \quad (24)$$

with $\rho = 2k_F^3/3\pi^2$.

In Fig. 3 we show the calculated results, solid, dashed and dot-dash lines, compared to experimental points from Ref. [19] for uranium and lead nuclei. The dash-dot line is obtained using a free pion propagator, in which case we observe that the isobar becomes too narrow to describe the width of the measured data, even with included smearing due to Fermi motion of the nucleons.

For the two other curves the dressed pion propagator was taken from the result of a self-consistent calculation based on the pion-nucleon scattering amplitude, Ref. [20]. We also checked that using a pion propagator from some other computations, i.e. from Ref. [6] and Ref. [18] does not produce significantly different results (with small adjustments of form-factor cutoffs). Actually, using a non self-consistently calculated pion propagator needs a softer form factor (21) because of the more pronounced strength of the particle-hole branch. The mentioned latter two curves, solid and dashed line, show the sensitivity to the $\Lambda_{\pi N\Delta}$ cut-off in the $\pi N\Delta$ vertex, the solid line corresponding to $\Lambda_{\pi N\Delta} = 0.7$ GeV and the dashed line to $\Lambda_{\pi N\Delta} = 0.8$ GeV. In both cases a πNN form factor with $\Lambda_{\pi NN} = 0.5$ GeV was used and we introduced a mean-field shift of the isobar mass (relative to that of the nucleon) of -30 MeV, to better match the position of the experimental peak. The need for very soft πNN form factor we attribute to the properties of the calculational scheme of Ref. [20], in which case no form factor was used in the computation of the loop integrals, determining the self energy of nucleon excitations. We did not include a form factor for the $\gamma N\Delta$ vertex, which would affect little the basic shape of the curves, only introducing some suppression at photon energies larger than 0.3 GeV. Subtraction of the background of the experimental points was not attempted. The relative importance of the background is expected to increase with leaving the central part of the isobar resonance.

In Fig. 4 we show the isobar spectral function (helicity-1/2 and helicity-3/2 components) in the nuclear medium for different momenta, for parameter values leading to the solid line in Fig. 3. We observe a non-negligible splitting between the two helicity states and the width is, though increasing with momentum, not very different from that in vacuum. The positions of the maxima are shifted with respect to the vacuum case by slightly less than the introduced -30 MeV mean-field shift. More detailed examination of the momentum dependence of the two helicities shows that their splitting is relatively small below $|\vec{p}| = 200$ MeV, reaches maximum around 300 MeV and then decreases with increasing momentum, becoming again small above 900 MeV.

IV. CONCLUSION

We studied the in-medium behavior of the isobar, using a relativistically covariant approach for describing its self energy and propagator. A convenient basis is provided by the subset of terms used for the in-medium generalization of the partial-wave expansion introduced in Ref. [10]. Using a generalized pion-nucleon-isobar vertex that allows for spin-1/2 components we observed a small (on the order of a few percent of the spin-3/2 spectral function) presence of spin-1/2 components both in vacuum and in nuclear matter of saturation density. In the nuclear medium the two helicity states appear with different spectral functions at nonzero isobar momentum (in the rest frame of the medium).

The dominance of the spin-3/2 states allows a much simplified, approximate calculation (not used in the present case) with only one component in the vacuum (when the two helicity states are degenerate) and two components in the medium with high precision, if the density of the medium does not significantly exceed the saturation density. Actually it suffices to calculate the relevant one or two components of the self energy to obtain the appropriate components of the dressed propagator. Physical quantities are expressed in terms of these propagator components. These considerations apply to the energy region where the isobar resonance is prominent, further off shell the non-spin-3/2 terms in the propagator may become sizable compared to the spin-3/2 components.

Computation of the total photo-absorption cross section on the free and in-medium nucleon in the isobar region shows reasonable agreement with the data, even without introducing a form factor for the photon-nucleon-isobar

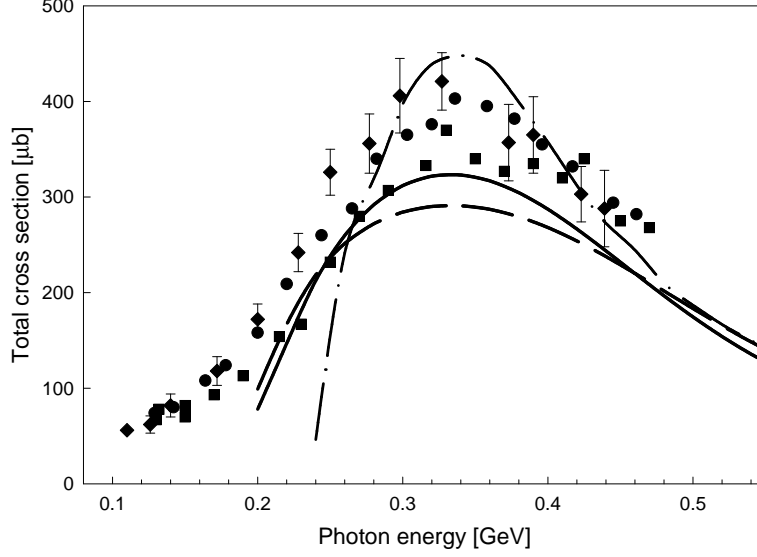


FIG. 3: The total photoabsorption cross section on an in-medium nucleon at saturation density. The dash-dot line is based on the free pion propagator. The other two curves have been calculated using the pion propagator from Ref. [20] with $g'_{NN} = 0.8$, $g'_{N\Delta} = g'_{\Delta\Delta} = 0.6$. For the solid line the form-factor cutoffs are: $\Lambda_{\pi NN} = 0.5$ GeV, $\Lambda_{\pi N\Delta} = 0.7$ GeV, while for the dashed line $\Lambda_{\pi NN} = 0.5$ GeV, $\Lambda_{\pi N\Delta} = 0.8$ GeV. When using the dressed pion propagator a mean-field shift of -30 MeV has been introduced for the isobar mass. No form factor has been used for the $\gamma N\Delta$ vertex. The experimental points are from Ref. [19] for uranium and lead.

vertex. In the medium one has to take into account the dressing of the pion propagator, which leads to an additional broadening of the isobar, mainly due to the particle-hole excitation. This broadening is reduced by the use of an off-shell pion-nucleon-isobar form factor. The required cut-off for the exponential form of (21) turns out to be $5-6 m_\pi$.

Acknowledgments

This work is part of the research program of the “Stichting voor Fundamenteel Onderzoek der Materie” (FOM) with financial support from the “Nederlandse Organisatie voor Wetenschappelijk Onderzoek” (NWO). C.L.K would like to thank the NWO for providing a visitors stipend and the K.V.I. (Groningen) for the kind hospitality. The authors would like to thank Olaf Scholten for useful discussions.

APPENDIX A

The nonzero expansion coefficients of the inverse of the free isobar propagator, Eq. (13), are given for $p^2 > 0$ by:

$$\begin{aligned}
 g_{[11]}^{(Q)-1} &= \sqrt{p^2} - M, & g_{[22]}^{(Q)-1} &= -(\sqrt{p^2} + M), \\
 g_{[11]}^{(P)-1} &= 2(\sqrt{p^2} + M), & g_{[13]}^{(P)-1} &= \sqrt{3}M \\
 g_{[22]}^{(P)-1} &= -2(\sqrt{p^2} - M), & g_{[24]}^{(P)-1} &= -\sqrt{3}M \\
 g_{[31]}^{(P)-1} &= \sqrt{3}M, & g_{[42]}^{(P)-1} &= -\sqrt{3}M \\
 g_{[55]}^{(P)-1} &= \sqrt{p^2} - M, & g_{[66]}^{(P)-1} &= -(\sqrt{p^2} + M),
 \end{aligned} \tag{A1}$$

with M being the bare mass of the isobar.

The expansion coefficients, $\sigma_{[ij]}^{(Q)}$ and $\sigma_{[ij]}^{(P)}$, of the isobar self energy form a symmetric 2×2 and a symmetric 6×6

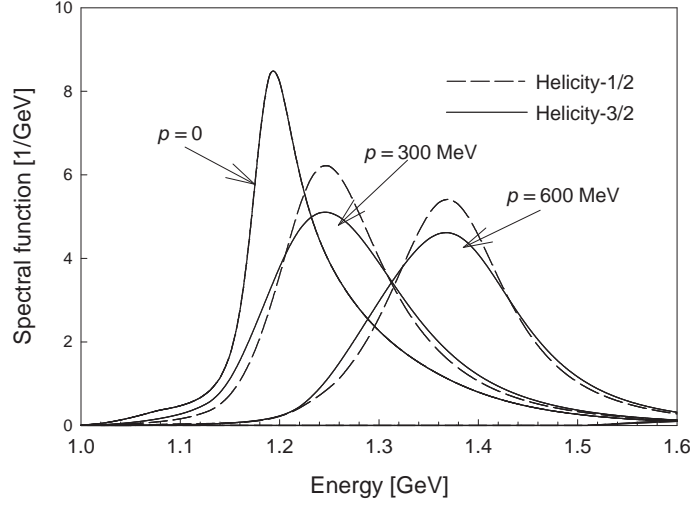


FIG. 4: The isobar spectral function in the medium, calculated using the pion propagator from Ref. [20] and with $\Lambda_\pi = 0.6$ GeV (leading to the solid line in Fig. 3). The dashed line shows the helicity-1/2 and the solid line the helicity-3/2 component. The three groups of curves, from left to right, correspond to momenta $|\vec{p}| = 0$, $|\vec{p}| = 300$ MeV and $|\vec{p}| = 600$ MeV.

matrix, with entries given for $i \leq j$ by:

$$\begin{aligned}
\sigma_{[11]}^{(Q)} &= M_N L_3 + L_7, \\
\sigma_{[12]}^{(Q)} &= -i L_8, \\
\sigma_{[22]}^{(Q)} &= M_N L_3 - L_7, \\
\sigma_{[11]}^{(P)} &= \frac{1}{3} [M_N (2L_3 - L_5) - 2L_7 + L_{12}], \\
\sigma_{[12]}^{(P)} &= \frac{i}{3} (-2L_8 + L_{11}), \\
\sigma_{[13]}^{(P)} &= \frac{1}{\sqrt{3}} [-\sqrt{p^2} (2L_3 - L_5) + 2L_7 - L_{12}], \\
\sigma_{[14]}^{(P)} &= \frac{i}{\sqrt{3}} [M_N (\sqrt{p^2} L_2 - L_6) - \sqrt{p^2} L_6 + L_{10}], \\
\sigma_{[15]}^{(P)} &= \frac{i\sqrt{2}}{3} (2L_8 - L_{11}), \\
\sigma_{[16]}^{(P)} &= \frac{\sqrt{2}}{3} [M_N (L_3 + L_5) - L_7 - L_{12}], \\
\sigma_{[22]}^{(P)} &= \frac{1}{3} [M_N (2L_3 - L_5) + 2L_7 - L_{12}], \\
\sigma_{[23]}^{(P)} &= \frac{i}{\sqrt{3}} [M_N (\sqrt{p^2} L_2 - L_6) - \sqrt{p^2} L_6 - L_{10}], \\
\sigma_{[24]}^{(P)} &= \frac{1}{\sqrt{3}} [-\sqrt{p^2} (2L_3 - L_5) + 2L_7 - L_{12}], \\
\sigma_{[25]}^{(P)} &= \frac{\sqrt{2}}{3} [M_N (L_3 + L_5) + L_7 + L_{12}], \\
\sigma_{[26]}^{(P)} &= \frac{i\sqrt{2}}{3} (2L_8 - L_{11}),
\end{aligned}$$

$$\begin{aligned}
\sigma_{[33]}^{(P)} &= M_N p^2 L_0 + (p^2 - 2M_N \sqrt{p^2}) L_1 + (M_N - 2\sqrt{p^2}) L_4 + L_9, \\
\sigma_{[34]}^{(P)} &= i(-p^2 L_2 + 2\sqrt{p^2} L_6 - L_{10}), \\
\sigma_{[35]}^{(P)} &= i\sqrt{\frac{2}{3}} \left[-M_N \sqrt{p^2} L_2 + (M_N - \sqrt{p^2}) L_6 + L_{10} \right], \\
\sigma_{[36]}^{(P)} &= \sqrt{\frac{2}{3}} \left[-\sqrt{p^2} (L_3 + L_5) + L_7 + L_{12} \right], \\
\sigma_{[44]}^{(P)} &= M_N p^2 L_0 - (p^2 + 2M_N \sqrt{p^2}) L_1 + (M_N + 2\sqrt{p^2}) L_4 - L_9, \\
\sigma_{[45]}^{(P)} &= \sqrt{\frac{2}{3}} \left[-\sqrt{p^2} (L_3 + L_5) + L_7 + L_{12} \right], \\
\sigma_{[46]}^{(P)} &= i\sqrt{\frac{2}{3}} \left[-M_N \sqrt{p^2} L_2 + (M_N + \sqrt{p^2}) L_6 - L_{10} \right], \\
\sigma_{[55]}^{(P)} &= \frac{1}{3} [M_N (L_3 - 2L_5) + L_7 - 2L_{12}], \\
\sigma_{[56]}^{(P)} &= \frac{i}{3} (5L_8 + 2L_{11}), \\
\sigma_{[66]}^{(P)} &= \frac{1}{3} [M_N (L_3 - 2L_5) - L_7 + 2L_{12}].
\end{aligned} \tag{A2}$$

The pion-nucleon loop integrals L_i ($i = 0, \dots, 12$) are regularized by the form factor present in the pion-nucleon-isobar vertex. The imaginary part of the loop integrals is first computed from the imaginary parts of the nucleon and pion propagator and with the help of the form factor made to approach zero at large energy. The real part is then computed from a convergent dispersion integral. For the nucleons we use a Fermi-gas description, while the pion propagator can be any result, obtained in an independent calculation.

The imaginary part of the loop integrals is then given by the following expression:

$$\text{Im } L_i(p, u) = \frac{g_{\pi N \Delta}^2}{8\pi^2} \int_{k_F}^{\infty} \frac{k^2 dk}{E_k} \int_{-1}^1 d\mu F(p, k)^2 \text{Im} \left[D_\pi(p_0 - E_k, |\vec{p} - \vec{k}|) \right] K_i(p, k), \tag{A3}$$

where $F(p, k)$ is the $\pi N \Delta$ form factor, $\mu \equiv \cos \theta(\vec{p}, \vec{k})$, D_π the pion propagator and the functions $K_i(p, k)$ are:

$$\begin{aligned}
K_0 &= 1, & K_1 &= k \cdot \hat{p}, & K_2 &= -X \cdot k, & K_3 &= \frac{1}{2} [M_N^2 - (k \cdot \hat{p})^2 + (X \cdot k)^2], \\
K_4 &= (k \cdot \hat{p})^2, & K_5 &= (X \cdot k)^2, & K_6 &= -(X \cdot k)(k \cdot \hat{p}), \\
K_7 &= (k \cdot \hat{p})K_3, & K_8 &= -(X \cdot k)K_3, & K_9 &= (k \cdot \hat{p})^3, \\
K_{10} &= -(X \cdot k)(k \cdot \hat{p})^2, & K_{11} &= -(X \cdot k)^3, & K_{12} &= (k \cdot \hat{p})(X \cdot k)^2,
\end{aligned} \tag{A4}$$

with $k \cdot \hat{p} \equiv k \cdot p / \sqrt{p^2}$ and $X \equiv X(p, u)$ defined in Eq. (4).

APPENDIX B

The terms $a_{[ij]}^{(Q)}(k, q)$ and $a_{[ij]}^{(P)}(k, q)$ in Eq. (19) are symmetric under the exchange of i and j , thus we give them only for $i \leq j$. Defining $M_\pm \equiv M_N \pm k \cdot p / \sqrt{p^2}$ and writing simply X_μ for $X_\mu(p, u)$, the nonzero values are as follows:

$$\begin{aligned}
a_{11}^{(Q)} &= \frac{p^2}{2} M_+ \left[-M_+ M_- + (X \cdot k)^2 \right], \\
a_{12}^{(Q)} &= \frac{-ip^2}{2} (X \cdot k) \left[M_+ M_- - (X \cdot k)^2 \right], \\
a_{22}^{(Q)} &= \frac{p^2}{2} M_- \left[-M_+ M_- + (X \cdot k)^2 \right], \\
a_{11}^{(P)} &= \frac{-2p^2}{3} M_+ M_-^2,
\end{aligned}$$

$$\begin{aligned}
a_{12}^{(P)} &= \frac{2ip^2}{3} M_+ M_- (X \cdot k), \\
a_{15}^{(P)} &= \frac{i\sqrt{2}p^2}{3} M_+ M_- (X \cdot k), \\
a_{16}^{(P)} &= \frac{\sqrt{2}p^2}{2} M_- \left[\frac{1}{3} M_+ M_- + (X \cdot k)^2 \right], \\
a_{22}^{(P)} &= \frac{-2p^2}{3} M_+^2 M_-, \\
a_{25}^{(P)} &= \frac{\sqrt{2}p^2}{2} M_+ \left[\frac{1}{3} M_+ M_- + (X \cdot k)^2 \right], \\
a_{26}^{(P)} &= \frac{i\sqrt{2}p^2}{3} M_+ M_- (X \cdot k), \\
a_{55}^{(P)} &= \frac{-p^2}{2} M_+ \left[\frac{5}{3} M_+ M_- + (X \cdot k)^2 \right], \\
a_{56}^{(P)} &= -i \frac{(X \cdot k)}{2} p^2 \left[\frac{7}{3} M_+ M_- + 3 (X \cdot k)^2 \right], \\
a_{66}^{(P)} &= \frac{-p^2}{2} M_- \left[\frac{5}{3} M_+ M_- + (X \cdot k)^2 \right].
\end{aligned} \tag{B1}$$

We note that all terms containing index 3 or 4 are identically zero.

-
- [1] W. Rarita and J. Schwinger, Phys. Rev. **60**, 61 (1941).
 - [2] R. M. Davidson, N. C. Mukhopadhyay, and R. S. Wittmann, Phys. Rev. D **43**, 71 (1991).
 - [3] V. Pascalutsa, Phys. Rev. D **58**, 096002 (1998).
 - [4] V. Pascalutsa and R. Timmermans, Phys. Rev. C **60**, 042201 (1999).
 - [5] V. Pascalutsa, Phys. Lett. B **503**, 85 (2001).
 - [6] C. L. Korpa and R. Malfliet, Phys. Rev. C **52**, 2756 (1995).
 - [7] F. de Jong and R. Malfliet, Phys. Rev. C **46**, 2567 (1992).
 - [8] L. Xia, P. J. Siemens, and M. Soyeur, Nucl. Phys. A **578**, 493 (1994).
 - [9] L. V. Daele, A. Y. Korchin, D. V. Neck, O. Scholten, and M. Waroquier, Phys. Rev. C **65**, 014613 (2002).
 - [10] M. F. M. Lutz and C. L. Korpa, Nucl. Phys. A **700**, 309 (2002).
 - [11] C. L. Korpa, Heavy Ion Phys. **5**, 77 (1997).
 - [12] A. E. Kaloshin and V. P. Lomov, Mod. Phys. Lett. A **19**, 135 (2004).
 - [13] V. Pascalutsa and D. R. Phillips, Phys. Rev. C **67**, 055202 (2003).
 - [14] T. A. Armstrong, W. R. Hogg, G. M. Lewis, A. W. Robertson, G. R. Brookes, A. S. Clough, J. H. Freeland, W. Galbraith, A. F. King, W. R. Rawlinson, et al., Phys. Rev. D **5**, 1640 (1972).
 - [15] H. F. Jones and M. D. Scadron, Ann. Phys. **81**, 1 (1973).
 - [16] W. Koepf, L. L. Frankfurt, and M. Strikman, Phys. Rev. D **53**, 2586 (1996).
 - [17] E. Oset, H. Toki, and W. Weise, Phys. Rep. **83**, 281 (1982).
 - [18] M. F. M. Lutz, Phys. Lett. B **552**, 159 (2003).
 - [19] J. Ahrens, J. Arends, P. Bourgeois, P. Carlos, J. L. Fallou, N. Floss, P. Garganne, S. Huthmacher, U. Kneissl, G. Mank, et al., Phys. Lett. B **146**, 303 (1984).
 - [20] C. L. Korpa and M. F. M. Lutz, nucl-th/0306063.